analytical chemistry

Article

pubs.acs.org/ac

Rational Design of a Bisphenol A Aptamer Selective Surface-Enhanced Raman Scattering Nanoprobe

Haley L. Marks,*[,†] Michael V. Pishko,[†] George W. Jackson,[‡,§] and Gerard L. Coté[†]

[†]Department of Biomedical Engineering, Texas A&M University, College Station, Texas 77843, United States

[‡]BioTex, Incorporated, Houston, Texas 77054, United States

[§]Base Pair Biotechnologies, Incorporated, Pearland, Texas 77584, United States

Supporting Information

ABSTRACT: Surface-enhanced Raman scattering (SERS) optical nanoprobes offer a number of advantages for ultrasensitive analyte detection. These functionalized colloidal nanoparticles are a multifunctional assay component. providing a platform for conjugation to spectral tags, stabilizing polymers, and biorecognition elements such as aptamers or antibodies. We demonstrate the design and characterization of a SERS-active nanoprobe and investigate the nanoparticles' biorecognition capabilities for use in a competitive binding assay. Specifically, the nanoprobe is designed for the quantification of bisphenol A (BPA) levels in the blood after human exposure to the toxin in food and beverage plastic packaging. The nanoprobes demonstrated specific affinity to a BPA aptamer with a dissociation constant K_d of 54 nM, and provided a dose-dependent SERS spectra with a limit of detection of 3 nM. Our conjugation approach shows the versatility of colloidal nanoparticles in assay development, acting as detectable spectral tagging elements and biologically active ligands concurrently.

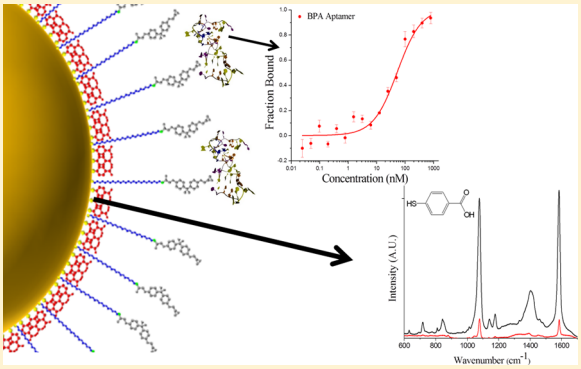

Raman scattering techniques have emerged as a unique tool in the development of blood biomarker assays in providing characteristic chemical fingerprints, low limits of detection, and capability for multiplexing due to narrow band widths.[1] The Raman signal stems from the inelastic scattering of photons by a molecule's electric cloud, providing a chemical fingerprint of the analyte. Only about 1 in 10^8 incident photons undergoes spontaneous Raman scattering, consequently causing the technique's intrinsically weak signal. In surface-enhanced Raman spectroscopy (SERS) electromagnetic enhancements are observed when the analyte is in close proximity to a plasmonic surface such as metallic colloidal nanoparticles.[2−5] In colloidal SERS, this leads to signal enhancements of up to 10^{11} when the analyte is sandwiched within 1 nm of two gold spherical particles.[6,7] Nevertheless, SERS techniques utilizing nanoparticles often lack reproducibility and specificity due to the random nature of particle aggregation and the adsorption of molecules onto the metal surface,[3] making it difficult to obtain quantitative analyte information. The integration of SERS detection with biomolecular assays has been recently implemented through the design of SERS nanoprobes: metallic nanoparticles conjugated to molecules with specific optical and biochemical functionalities.[8−10]

SERS nanoprobes require three key conjugated elements: (1) a Raman reporter molecule (RRM) for quantitative identification, (2) a protective element for particle stabilization, and (3) a ligand for assay-specific biorecognition.[8] Strong Raman bands are attributed to RRMs with a high Raman cross section, meaning the molecule's electron cloud is easily distorted by the excitation laser and thus is polarizable.[11,12] In order to reduce the *number* of Raman bands for simplified spectral multiplexing, the RRM should also have a low atom count and/or be highly symmetrical.[13−16] Furthermore, the RRM must provide a functional "head" group for chemisorption to the nanoparticle, most commonly chosen as a thiol (R−SH) for its well-defined covalent attachment to gold.[17,18] Formation of a self-assembled monolayer (SAM) of RRMs on the nanoparticle surface allows for dense packing of molecules with uniform orientation, improving the reproducibility of the SERS signal.[14,19−21] The RRM's terminal "tail" group type also contributes to the dynamics of the nanoparticles as its charge directly affects the total particle surface charge, determining the degree of electrostatic stabilization.[22,23]

Though a Raman reporter SAM can independently act as the nanoprobe's stabilizing capping agent, additional *steric* stabilization is often desired for mechanical repulsion between particles. Conjugation of polymers such as poly(ethylene) glycol (PEG)[24−27] or poly(vinylpyrrolidone) (PVP)[14,28,29] to the nanoparticle as part of a mixed SAM, to the RRM's "tail" group,

Received: July 10, 2014
Accepted: October 20, 2014
Published: October 20, 2014

or silica shell encapsulation[14,30] of the particles drastically improves the colloid's shelf life, even under harsh conditions. Sterically stabilized nanoprobes exhibit minimal nonspecific adsorption and can also provide functionalized surfaces and binding sites for further bioconjugation.

To provide a molecular affinity to the SERS nanoprobe, a biorecognition element (i.e., an antigen or antibody) must also be conjugated to the particle, via a thiol to the gold directly, to the RRM, or to the protective linker. Recently, *aptamers*, highly specific and sensitive affinity molecules derived from nucleic acids, have been used as SERS nanoprobe recognition ligands in lieu of typical antibodies.[31−37] Aptamers are specifically advantageous for sensing small molecules with low immunogenicity, where raising antibodies would require synthesis of a hapten−target carrier before animals can be immunized with that conjugate.[38] Selection of aptamers is an entirely in vitro process with the ability to perform counterselection steps and/or selection under nonblood conditions. This provides the potential for greater ligand specificity and affinity, and once identified, aptamers are readily produced by scalable chemical synthesis. Lastly, aptamer terminal functional groups are readily incorporated during synthesis for conjugation to the nanoparticle or other immobilization assay steps.[39]

Aptamers are well-suited for the detection of environmental carcinogens in the blood, where animal immunizations with certain toxic haptens are not possible or do not trigger an animal immune response.[40] Bisphenol A (BPA) is the monomer of an epoxy resin commonly used in plastic food and beverage packaging, and can be toxic to the endocrine system when exposed to humans. Though environmental monitoring of BPA in the air, water, and the food products themselves is well-established and regulated, there is still a need for reliable human biomonitoring methods in order to determine the body's burden with BPA and its metabolites in the blood.

In this work a functional SERS nanoprobe with specific affinity to a BPA-binding aptamer is characterized. The binding affinity of the nanoprobe and its specificity to the BPA aptamer is quantified using microscale thermophoresis (MST). This approach monitors the signal depletion of a fluorescently labeled aptamer as it moves along an induced temperature gradient.[41,42] The thermophoresis of molecules is size-dependent, and thus titration experiments are used to quantify the aptamer−nanoparticle binding and determine the dissociation constant K_d. The plasmonic properties of these capture nanoprobes and their capabilities for quantitative SERS detection are also investigated. We demonstrate that the described SERS nanoprobes are capable of acting as both a capture and detecting element for BPA assay development.

EXPERIMENTAL METHODS

According to the scheme in Figure 1, the nanoprobe consists of a RRM and heterobifunctional PEG mixed SAM conjugated to a BPA derivative, bisphenol A diglycidyl ether (BADGE). The design of the nanoprobe, reliable reaction conditions for its repeatable production, and ratios of conjugates were optimized. Additionally, the affinity behavior of a BPA aptamer to the BADGE SERS nanoprobe was characterized using MST. The ability to detect and quantify these capture nanoprobes using SERS was explored, though aggregation of the particles was required to reach the particle concentration range of interest.

Materials. Citrate-reduced colloidal gold nanoparticles with an average diameter of 60 nm were purchased from

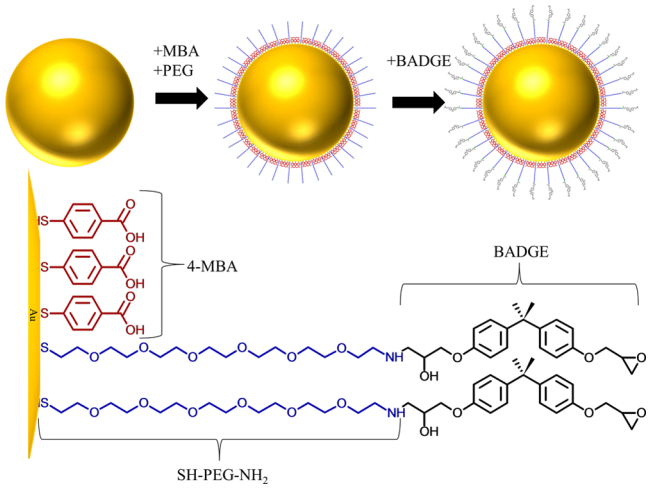

Figure 1. Scheme for the synthesis of BADGE-functionalized SERS nanoprobes. Below: chemical structures of mixed SAM components.

Polysciences (no. 22717). Heterobifunctional PEG linker (NH_2−PEG−SH) with a molecular weight of 1 kDa was purchased from NanoCS. Bisphenol A diglycidyl ether (BADGE), 4-mercaptobenzoic acid (4-MBA), 4-(2-hydroxyethyl)piperazine-1-ethanesulfonic acid (HEPES), and 200 proof ethanol (EtOH) were obtained from Sigma-Aldrich. The BPA-specific aptamer 5′-CCG CCG TTG GTG TGG TGG GCC TAG GGC CGG CGG CGC ACA GCT GTT ATA GAC GTC TCC AGC-3′[43] was synthesized with a 5′-Cy5 fluorescent dye by Eurofins Genomics (Ebersberg, Germany). Similarly, nonspecific aptamers were also obtained from Eurofins. Milli-Q ultrapure water (18 MΩ) was used in all procedures.

Characterization. Transmission electron microscopy (TEM) images were acquired on a JEM-2010 TEM (JEOL, Japan) system. UV−vis−NIR extinction spectra were recorded by a Tecan Infinite 200 Pro (Tecan Group Ltd., Switzerland) microplate reader with a scan range of 400−900 nm, using 300 μL of each sample in a 96-well plate. The ζ-potential and hydrodynamic diameters of the nanoparticles were measured on a Zetasizer Nano ZS90 (Malvern, U.K.). All Raman and SERS spectra were collected using a Thermo Scientific DXR Raman confocal microscope. A 396-well plate (30 μL of sample per well) was used for all liquid SERS measurements. Samples were excited with a 5 mW, 780 nm laser through a 10× microscope, using an exposure time of 5 s, where each scan comprises 30 exposures. Microscale thermophoresis data sets were collected using a NanoTemper MST system at 2Bind Molecular Interactions (2Bind, Germany).

Au/MBA/PEG/BADGE SERS Nanoprobe Synthesis. To synthesize 1 mL of nanoprobes, 10 μL of HEPES buffer (1 M at pH ∼9) was first added to 1 mL of 60 nm gold nanoparticles (∼24 pM stock solution, where nanoparticle concentrations are calculated by Beer−Lamberts' law using the measured absorbance of the nanoparticles and an extinction coefficient of 5.32×10^{10} M^{-1} s^{-1}). Nanoparticle characterization of the stock gold colloid can be found for comparison in Figure 2. Solutions of the Raman reporter molecule 4-MBA (120 μL of 10 μM in 100% EtOH) and the linker NH_2−PEG−SH (80 μL of 10 μM in 10 mM HEPES at pH ∼9) were then added dropwise to 1 mL of the gold nanoparticle solution under vigorous stirring. The mixed SAM components were allowed to

dx.doi.org/10.1021/ac502541v | Anal. Chem. 2014, 86, 11614−11619

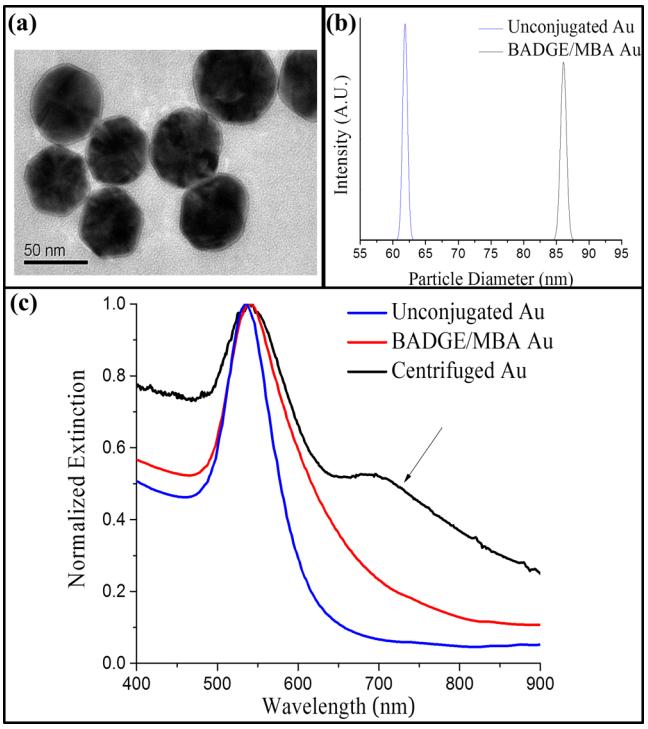

Figure 2. (a) TEM image of the conjugated gold nanoparticles; (b) size distribution of unconjugated gold (blue) and BADGE conjugated nanoprobes (black), measured by dynamic light scattering; (c) extinction spectra plotted vs wavelength for unconjugated gold (blue), BADGE conjugated gold nanoprobes (red), and centrifugally aggregated nanoprobes (black).

bind with the gold via their −SH terminal groups for 4 h, to ensure complete SAM formation.

Unbound reporter and linker molecules were removed by centrifuging the solution for 10 min at 4000 rpm and redispersing the precipitate in 10 mM HEPES buffer. BADGE was then conjugated to the nanoparticle via its epoxide, binding with the PEG linker's terminal amine group; 100 μL of 10 μM of BADGE in 10 mM HEPES was added dropwise to the nanoprobe solution under vigorous stirring and allowed to react overnight. The particles were then washed twice by centrifuging (4000 rpm/10 min) and resuspending the precipitate in a 40% EtOH/H_2O solution, followed by mild sonication. It was approximated that there are 7.5×10^4 Raman reporter molecules (4-MBA) and 5.0×10^4 aptamer binding molecules (BADGE) conjugated to each gold nanoparticle where the concentration of nanoparticles after conjugation is calculated to be 16 pM.

Microscale Thermophoresis Aptamer Binding Measurements. For MST measurements, a Monolith NT.115 Pico instrument (Nanotemper, Munich, Germany) was employed. Fifteen capillaries of the instrument were filled with 15 serial dilutions of the BADGE SERS nanoprobes starting from the stock particle concentration of 16 pM, corresponding to an estimated total solution BADGE concentration range of 800 nM to 20 pM. The BPA aptamer and unspecific aptamer concentrations were held constant in each capillary at 5 nM. A fluorescent measurement of the cold solution is made before turning the IR heating laser on (laser power 80%, LED power 15%, temperature 25 °C). Once the laser is on, the fluorescence in the capillary is measured as the aptamers/aptamer–nanoparticle conjugates move toward the colder outer walls of the capillary tubes. This fluorescent signal is used to quantify binding induced size changes, and the fraction of aptamer bound as a function of analyte concentration is calculated according to Baaske et al.[41] A technical replicate of each fluorescent measurement set was made. This experiment was repeated using 5 nM of the BPA-aptamer and 15 serial dilutions of BPA in free solution for a concentration range of 10 μM to 310 pM. The dissociation constants, or K_d, were calculated from the resulting sigmoidal curves using the built-in Hill1 sigmoidal fit in Origin 9.1

SERS Concentration Response Measurements. Ten serial dilutions of the BADGE SERS nanoprobes were performed starting from the stock concentration of 16 pM corresponding to the total solution BADGE concentration range of 800 nM to 40 pM and a total Raman reporter (4-MBA) concentration range of 1.2 μM to 60 pM. Nested centrifuge tubes were cut for easy integration with the Raman microscope system, and 100 μL of each dilution was centrifuged at 10 000 rpm for 10 min. The solution was removed, and the precipitate was allowed to dry overnight. The SERS intensity of the aggregates formed at the bottom of each tube was then measured in triplicate and averaged to represent the SERS response.

RESULTS AND DISCUSSION

SERS Nanoprobe Synthesis. The BADGE-functionalized SERS nanoprobes were synthesized according to scheme in Figure 1 and are composed of (1) mercaptobenzoic acid (4-MBA) acting as the RRM, (2) a heterobifunctional PEG linker providing steric stabilization and protection from unwanted adsorption, and (3) the analyte of interest, BADGE. TEM images of the BADGE SERS nanoprobes demonstrate an average particle diameter of ∼60 nm, and dynamic light scattering (DLS) measurements confirmed minimal aggregation after conjugation with an average particle diameter reading of 86.1 nm (Figure 2, parts a and b). The ζ-potential of the nanoprobes increased from −41.7 to −34.6 mV after the mixed SAM was formed, due to the presence of terminal amines on the PEG linker. After BADGE conjugation, epoxide groups replace the amines and the ζ-potential decreased to −44.0 mV, indicating adequate particle stabilization was achieved sterically by the PEG and electrostatically by the 4-MBA's terminal carboxylic acid group.[21,44]

Aptamer–Nanoparticle Binding. The binding analytics of the SERS nanoprobe to the BPA aptamer were quantified by the aptamer/target dissociation constant K_d, as determined by MST. Dilutions of the BADGE SERS nanoprobes, corresponding to 20 pM to 800 nM BADGE, were exposed to a constant 5 nM each of Cy5-labeled BPA aptamer and nonspecific aptamer. The aptamer–nanoparticle binding curves are shown in Figure 3, quantified as the fraction of the total solution concentration of fluorescent aptamer that is bound to SERS nanoprobes, as a function of total BADGE concentration present in the nanoparticle solution. The dissociation constant K_d was determined to be ∼54 nM for the BADGE nanoprobes, in comparison to 10 nM reported for free BPA binding to the same aptamer.[43] Additionally, the K_d value for free BPA binding to the BPA aptamer was determined experimentally using MST to be ∼100 nM (Supporting Information Figure S-1), further validating the usefulness of the capture nanoprobe for future competitive binding assay development. The control experiment using a nonspecific aptamer was negative (Figure 3),

dx.doi.org/10.1021/ac502541v | Anal. Chem. 2014, 86, 11614–11619

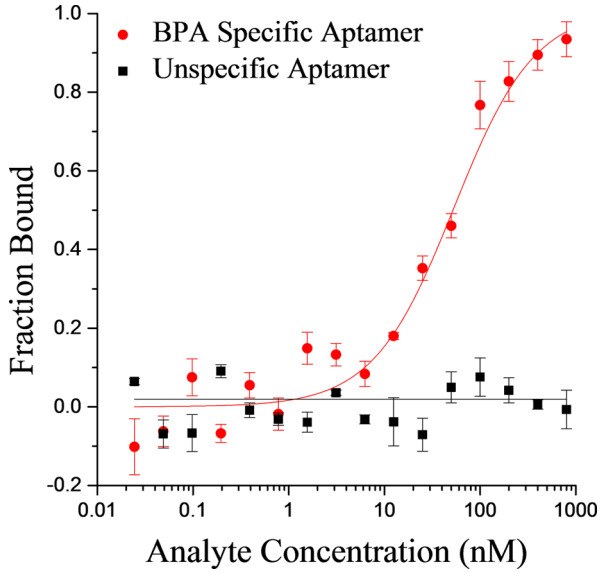

Figure 3. Binding behavior of the SERS nanoprobes to the published BPA-specific aptamer (red, $K_d \sim 54$ nM, $r^2 = 0.96$) and a non-BPA-specific aptamer (black) as measured by microscale thermophoresis (MST).

demonstrating that the SERS nanoprobes are specific to the BPA aptamer.

Plasmonic Properties of SERS Nanoprobes. The intrinsic signal enhancement provided by a SERS substrate relies heavily on the excitation of localized plasmons at the metallic surface by the Raman excitation laser.[11] This excitation of plasmons causes a shift in magnitude in the metallic nanoparticle extinction spectra, dependent on the size and stability of the particles.[5,45] The extinction profile is representative of the scattered light intensity as a function of excitation wavelength and, therefore, serves as a predictor of the magnitude of the relative SERS enhancement. In Figure 2c, the localized surface plasmon resonance (LSPR) extinction band for unconjugated gold nanoparticles is shown to be at 535 nm. After BADGE conjugation, the LSPR of the nanoparticles is slightly red-shifted to 540 nm, which can be attributed to the resultant increased particle diameter. Maximal SERS enhancements are observed when the LSPR falls within a 240 nm window including both the excitation wavelength and Raman-shifted wavelength,[2] specifically 780 ± 120 nm for the excitation laser used in this work. To shift their LSPR into this window and achieve the SERS enhancements needed for nanomolar detection, the nanoprobes were aggregated by centrifugation, and a secondary plasmon band at 700 nm becomes apparent in the extinction spectra, as indicated in Figure 2c.

The Raman spectra of the reporter molecule 4-MBA in powder form, the SERS spectra of the nanoprobes suspended in solution, and the SERS spectra of the nanoprobes after centrifugal aggregation are compared in Figure 4. The strongest characteristic vibrational modes for 4-MBA occur at ~1075 and 1586 cm^{-1}, corresponding to the C−H in-plane bending (β_{18b}) and C−C stretching (ν_{8a}) vibrational modes, respectively.[46−48] These bands are evident in the intrinsic Raman and nanoprobe SERS spectra (Figure 4), and are comparable to those previously reported for 4-MBA bound to gold.[14,20,30,47,49] Weaker Raman modes seen in the powdered 4-MBA spectrum become visible in the SERS signal when the nanoprobes are

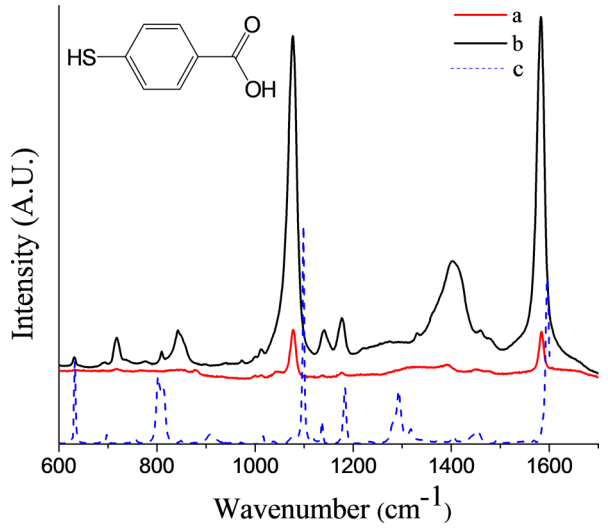

Figure 4. SERS signals of (a) 30 μL of nanoprobes suspended in solution and (b) 30 μL of nanoprobes aggregated by centrifugation, and (c) spontaneous Raman signal of the Raman reporter molecule (4-MBA) in powdered form. Inset: chemical structure of 4-MBA.

aggregated (Figure 4). Though some peaks are shifted or broadened, the strongest peaks in the SERS nanoprobe signature correspond to the published vibrational modes for 4-MBA (Table 1).

Table 1. Assignment of 4-MBA Vibrational Modes (cm^{-1}) to the Nanoprobe SERS Spectra

Raman (cm^{-1})	SERS (cm^{-1})	assignment[a]
697	718	γ(CCC)[b]
812	843	δ(COO−)[b]
1099	1075	β(C−H)[c,d]
1136	1141	β(C−H)[d]
1183	1177	β(C−H)[c,d]
1318	1330	ν_s(COO−)[b]
1404	1402	ν_s(COO−)[d]
1596	1586	ν(C−C)[c]

[a] δ = in-plane deformation, β = bending, γ = out-of-plane deformation, ν = stretching. [b]Ref 49. [c]Ref 46. [d]Ref 47.

SERS Response. The stock nanoprobe concentration was the lowest detectable concentration using SERS in solution phase. Therefore, 10 serial dilutions of the capture nanoprobes were centrifugally aggregated, dried, and their SERS spectra monitored to investigate the detection capabilities of the nanoprobes at the concentration range of interest (Figure 5a). Features assigned to the SERS nanoprobes' Raman reporter (4-MBA) dominate the spectra, until the concentration drops below ~10 nM and the area of aggregation becomes smaller than the laser spot size of 3.1 μm. At this point, peaks attributable to the polypropylene centrifuge tube background begin to dominate the spectra, while the SERS nanoprobe characteristic peaks at ~1075 and 1586 cm^{-1} decrease until they are no longer distinguishable after six serial dilutions (~1.10 nM, Figure 5a). The strongest polypropylene modes can be seen at 809 and 841 cm^{-1}, corresponding to the C−C−C in-plane ring deformation (α_1)[50,51] and C−H out-of-plane bending (γ_{10a})[51,52] vibrational modes, respectively.

The SERS peak intensities of the vibrational modes at 1075 and 1586 cm^{-1} as a function of concentration are shown in

dx.doi.org/10.1021/ac502541v | Anal. Chem. 2014, 86, 11614−11619

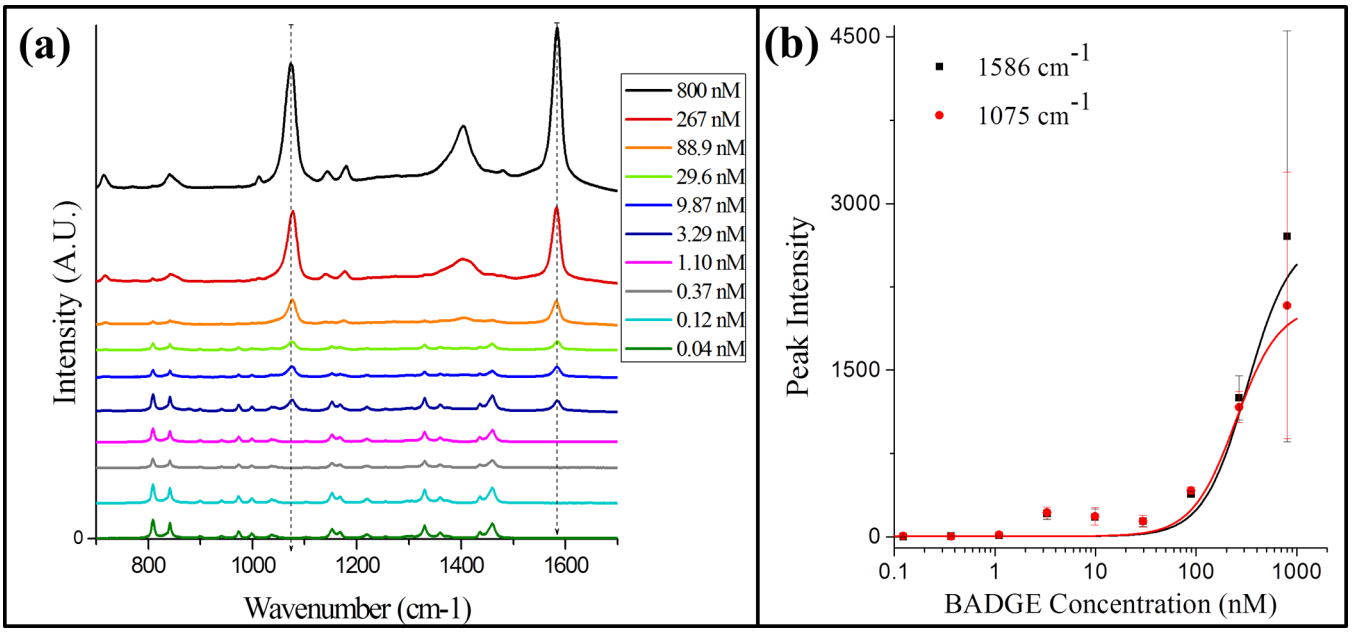

Figure 5. (a) SERS signals of 100 μL of centrifugally aggregated nanoprobes at 10 concentrations ranging from 40 pM to 800 nM, offset for clarity. (b) SERS intensity of the vibrational modes at 1075 and 1586 cm^{-1} with increasing volume of nanoprobes.

Figure 5b. The trend follows a typical dose−response curve, where the MBA peaks can be identified with a coefficient of variation <25%, until the nanoparticle concentration drops below 600 fM (3.29 nM BADGE). This sensitivity is competitive with the quantification limits previously reported for the detection of BPA levels in human blood utilizing liquid chromatography (LC)−tandem mass spectrometry, ranging from 0.43[53] to 64 nM.[54] It is noted that the standard error increases with increasing concentration, likely due to the nonhomogeneous nature of the aggregate formed using this method. For lower concentrations, centrifugation causes the small volume of particles to distribute evenly on the bottom of the tube. However, for higher volumes with a visible precipitate, a higher density of nanoparticle junctions[45] is formed, resulting in more areas of increased SERS enhancements.[11] Therefore, the analytical range for this method is ∼3−300 nM. Though this detection method for true quantitative analysis is impaired by high error from "hot spots", this proof-of-concept study demonstrates that limited concentration information may be obtained using SERS through the controlled aggregation of nanoparticles combined with PEGylation and conjugation of the Raman reporter to the nanoparticle as a self-assembled monolayer.

The limit of detection can be reduced and the analytical range shifted to suit a specific BPA aptamer assay through altering the ratio and amount of PEG linker and Raman reporter molecule conjugated to each particle. Modifying the amount or type of RRM directly affects the SERS signal intensity, while adjustments made to the PEG linker can be used to modify the distance between the particle and analyte, to reduce charge based interactions with the nanoparticle surface, or to alter the number of target analyte molecules per particle.[26] The binding affinity of the aptamer to the functionalized SERS nanoprobes may also be adjusted by changing the BPA derivative[55] or synthesizing a BADGE derivative with only one epoxy group so that its structure more closely resembles BPA.

CONCLUSION

This is the first report of the successful design of a functionalized SERS nanoparticle for specific binding to a BPA aptamer with an affinity similar to that of the analyte in free solution. The particles provide a characteristic Raman signature which can be enhanced through nanoparticle aggregation and detected by SERS at concentrations as low as 600 fM. The nanoprobes demonstrate colloidal stability for biological interaction while providing functional conjugation to the BADGE analyte. The aptamer/nanoprobe binding event is characterized through MST fluorescence measurements and quantified by a dissociation constant of 54 nM. This demonstrates the sensitive aptamer recognition capabilities of capture analytes immobilized onto SERS-active nanoparticles with minimal perturbation of the aptamer's native, free-analyte binding.

ASSOCIATED CONTENT

Supporting Information

Additional information as noted in text. This material is available free of charge via the Internet at http://pubs.acs.org.

AUTHOR INFORMATION

Corresponding Author

*E-mail: hmarks@tamu.edu.

Notes

The authors declare no competing financial interest.

ACKNOWLEDGMENTS

The authors acknowledge the financial support of the National Science Foundation CBET-1133512 and the National Institutes of Health SBIR 1R43ES022303-01. The authors also thank Dr. Thomas Schubert (2Bind, Regensburg, Germany) for conducting the microscale thermophoresis studies, Javier Garza (Optical BioSensing Lab, Texas A&M) for his help with SERS substrate fabrication, and Remington Harwell (Texas A&M) for capturing TEM images.

REFERENCES

(1) Gellner, M.; Schutz, M.; Salehi, M.; Packeisen, J.; Strobel, P.; Marx, A.; Schmuck, C.; Schlucker, S. *Proc. SPIE* **2010**, *7757*, 77570M.
(2) Willets, K. A.; Van Duyne, R. P. *Annu. Rev. Phys. Chem.* **2007**, *58*, 267.
(3) Kneipp, K.; Kneipp, H.; Manoharan, R.; Hanlon, E. B.; Itzkan, I.; Dasari, R. R.; Feld, M. S. *Appl. Spectrosc.* **1998**, *52*, 1493.
(4) Moskovits, M. *Rev. Mod. Phys.* **1985**, *57*, 783.
(5) Rechberger, W.; Hohenau, A.; Leitner, A.; Krenn, J. R.; Lamprecht, B.; Aussenegg, F. R. *Opt. Commun.* **2003**, *220*, 137.
(6) Kneipp, K.; Kneipp, H.; Itzkan, I.; Dasari, R. R.; Feld, M. S. *J. Phys.: Condens. Matter* **2002**, *14*, R597.
(7) Etchegoin, P. G.; Lacharmoise, P. D.; Le Ru, E. C. *Anal. Chem.* **2009**, *81*, 682.
(8) Wang, Y. L.; Schlucker, S. *Analyst* **2013**, *138*, 2224.
(9) Benford, M.; Wang, M.; Kameoka, J.; Good, T.; Cote, G. *Proc. SPIE* **2010**, *7577*, 757705.
(10) Chon, H.; Lim, C.; Ha, S. M.; Ahn, Y.; Lee, E. K.; Chang, S. I.; Seong, G. H.; Choo, J. *Anal. Chem.* **2010**, *82*, 5290.
(11) Ru, E. C. L.; Etchegoin, P. G. *Raman Spectroscopy and Related Optical Techniques*; Elsevier: Oxford, U.K., 2009.
(12) Wilson, E. B.; Decius, J. C.; Cross, P. C. *Molecular Vibrations: The Theory of Infrared and Raman Vibrational Spectra*; Dover Publications: New York, 1955.
(13) Faulds, K.; Jarvis, R.; Smith, W. E.; Graham, D.; Goodacre, R. *Analyst* **2008**, *133*, 1505.
(14) Gellner, M.; Kompe, K.; Schlucker, S. *Anal. Bioanal. Chem.* **2009**, *394*, 1839.
(15) Gracie, K.; Correa, E.; Mabbott, S.; Dougan, J. A.; Graham, D.; Goodacre, R.; Faulds, K. *Chem. Sci.* **2014**, *5*, 1030.
(16) Schlucker, S. *ChemPhysChem* **2009**, *10*, 1344.
(17) Jadzinsky, P. D.; Calero, G.; Ackerson, C. J.; Bushnell, D. A.; Kornberg, R. D. *Science* **2007**, *318*, 430.
(18) Love, J. C.; Estroff, L. A.; Kriebel, J. K.; Nuzzo, R. G.; Whitesides, G. M. *Chem. Rev.* **2005**, *105*, 1103.
(19) Barriet, D.; Yam, C. M.; Shmakova, O. E.; Jamison, A. C.; Lee, T. R. *Langmuir* **2007**, *23*, 8866.
(20) Orendorff, C. J.; Gole, A.; Sau, T. K.; Murphy, C. J. *Anal. Chem.* **2005**, *77*, 3261.
(21) Zhou, J.; Ralston, J.; Sedev, R.; Beattie, D. A. *J. Colloid Interface Sci.* **2009**, *331*, 251.
(22) Ulman, A. *Chem. Rev.* **1996**, *96*, 1533.
(23) Zhang, H.; He, H. X.; Wang, J.; Liu, Z. F. *Langmuir* **2000**, *16*, 4554.
(24) Jana, N. R.; Ying, J. Y. *Adv. Mater.* **2008**, *20*, 430.
(25) Jehn, C.; Kustner, B.; Adam, P.; Marx, A.; Strobel, P.; Schmuck, C.; Schlucker, S. *Phys. Chem. Chem. Phys.* **2009**, *11*, 7499.
(26) Jokerst, J. V.; Lobovkina, T.; Zare, R. N.; Gambhir, S. S. *Nanomedicine* **2011**, *6*, 715.
(27) McKenzie, F.; Ingram, A.; Stokes, R.; Graham, D. *Analyst* **2009**, *134*, 549.
(28) Moran, C. H.; Rycenga, M.; Zhang, Q.; Xia, Y. N. *J. Phys. Chem. C* **2011**, *115*, 21852.
(29) Papp, S.; Patakfalvi, R.; Dekany, I. *Croat. Chem. Acta* **2007**, *80*, 493.
(30) Kustner, B.; Gellner, M.; Schutz, M.; Schoppler, F.; Marx, A.; Strobel, P.; Adam, P.; Schmuck, C.; Schlucker, S. *Angew. Chem., Int. Ed.* **2009**, *48*, 1950.
(31) Barahona, F.; Bardliving, C. L.; Phifer, A.; Bruno, J. G.; Batt, C. A. *Ind. Biotechnol.* **2013**, *9*, 42.
(32) Li, M.; Zhang, J. M.; Suri, S.; Sooter, L. J.; Ma, D. L.; Wu, N. Q. *Anal. Chem.* **2012**, *84*, 2837.
(33) Oh, S.; Kim, M.; Kim, Y.; Jung, H.; Yoon, T. S.; Choi, Y. J.; Kang, C. J.; Moon, M. J.; Jeong, Y. Y.; Park, I. K.; Lee, H. H. *Appl. Phys. Lett.* **2013**, *103*, 083702.
(34) Pagba, C. V.; Lane, S. M.; Cho, H.; Wachsmann-Hogiu, S. *J. Biomed. Opt.* **2010**, *15*, 047006.
(35) Wen, G. Q.; Liang, A. H.; Jiang, Z. L. *Plasmonics* **2013**, *8*, 899.
(36) Yoon, J.; Choi, N.; Ko, J.; Kim, K.; Lee, S.; Choo, J. *Biosens. Bioelectron.* **2013**, *47*, 62.
(37) Yuan, Q.; Lu, D. Q.; Zhang, X. B.; Chen, Z.; Tan, W. H. *TrAC, Trends Anal. Chem.* **2012**, *39*, 72.
(38) Kuby, J. *Immunology*, 3rd ed.; W.H. Freeman: New York, 1997.
(39) Jayasena, S. D. *Clin. Chem.* **1999**, *45*, 1628.
(40) Moghaddam, A.; Løbersli, I.; Gebhardt, K.; Braunagel, M.; Marvik, O. J. *J. Immunol. Methods* **2001**, *254*, 169.
(41) Baaske, P.; Wienken, C. J.; Reineck, P.; Duhr, S.; Braun, D. *Angew. Chem., Int. Ed.* **2010**, *49*, 2238.
(42) Morris, M.; Baaske, P.; Langst, G.; Jackson, G. W. Presented at the Southwest Regional Meeting of the American Chemical Society, Baton Rouge, LA, 2012.
(43) Jo, M.; Ahn, J. Y.; Lee, J.; Lee, S.; Hong, S. W.; Yoo, J. W.; Kang, J.; Dua, P.; Lee, D. K.; Hong, S.; Kim, S. *Oligonucleotides* **2011**, *21*, 85.
(44) Israelachvili, J. *Intermolecular and Surface Forces*, 3rd ed.; Academic Press: Waltham, MA, 2010.
(45) Marimuthu, A.; Christopher, P.; Linic, S. *J. Phys. Chem. C* **2012**, *116*, 9824.
(46) Varsányi, G.; Láng, L.; Kovner, M. A. *Assignments for Vibrational Spectra of Seven Hundred Benzene Derivatives*; Institute of Physics Publishing: Bristol, U.K., 1974.
(47) Ma, W. Q.; Fang, Y.; Hao, G. L.; Wang, W. G. *Chin. J. Chem. Phys.* **2010**, *23*, 659.
(48) Wells, M.; Dermody, D. L.; Yang, H. C.; Kim, T.; Crooks, R. M.; Ricco, A. J. *Langmuir* **1996**, *12*, 1989.
(49) Michota, A.; Bukowska, J. *J. Raman Spectrosc.* **2003**, *34*, 21.
(50) Jasse, B.; Chao, R. S.; Koenig, J. L. *J. Polym. Sci., Polym. Phys. Ed.* **1978**, *16*, 2157.
(51) Sears, W. M.; Hunt, J. L.; Stevens, J. R. *J. Chem. Phys.* **1981**, *75*, 1589.
(52) Anema, J. R.; Brolo, A. G.; Felten, A.; Bittencourt, C. *J. Raman Spectrosc.* **2010**, *41*, 745.
(53) Markham, D. A.; Waechter, J. M., Jr.; Wimber, M.; Rao, N.; Connolly, P.; Chuang, J. C.; Hentges, S.; Shiotsuka, R. N.; Dimond, S.; Chappelle, A. H. *J. Anal. Toxicol.* **2010**, *34*, 293.
(54) Völkel, W.; Bittner, N.; Dekant, W. *Drug Metab. Dispos.* **2005**, *33*, 1748.
(55) Moreno, M. J.; D'Arienzo, P.; ManclúS, J. J.; Montoya, A. *J. Environ. Sci. Health, Part B* **2011**, *46*, 509.